Proceedings of the International Conference on Industrial Engineering and Operations Management

Publisher: IEOM Society International, USA DOI: 10.46254/AP07.20260199
Published: March 25, 2026

Performance Evaluation of Low-Cost MEMS Accelerometers for Machinery Vibration Monitoring: A Comparative Study with IEPE Sensors

Wetis Klingram
Master's Student, School of Industrial Engineering
Suranaree University of Technology
Nakhon Ratchasima, Thailand
m6701499@g.sut.ac.th

Nattawat Pinrath, Ph.D.
Lecturer, School of Industrial Engineering
Suranaree University of Technology
Nakhon Ratchasima, Thailand
nattawat.p@g.sut.ac.th

Abstract

Rotating machinery in industrial applications requires accurate vibration measurement for fault diagnosis and maintenance decision-making. IEPE sensors provide high accuracy, their cost limits large-scale deployment. This study evaluates the frequency, amplitude, harmonic, and noise performance of low-cost MEMS accelerometers in comparison with a reference IEPE sensor. Three MEMS accelerometers and one IEPE sensor were mounted on a vibration shaker and excited by sinusoidal signals in the 10–100 Hz range, with data simultaneously acquired at a sampling rate of 2 kHz. FFT-based analysis was applied to assess frequency tracking accuracy, narrowband RMS amplitude, harmonic detectability, noise floor, and signal-to-noise ratio (SNR). Additional experiments examined an electric motor under unbalanced conditions to examine practical applicability. The results indicate that the MEMS sensors achieve consistent sub-bin frequency tracking, with peak deviations remaining well below the theoretical FFT resolution ($\Delta f = 0.2$ Hz) for both fundamental and harmonic components. However, the narrowband RMS amplitude shows frequency-dependent deviations of up to approximately ±50–70% relative to the IEPE reference, and the SNR of the MEMS sensors (25–35 dB) is lower than that of the IEPE (>40 dB). These findings demonstrate strong potential for frequency-based condition monitoring, while accurate amplitude evaluation requires calibration.

Keywords
MEMS accelerometer, Vibration analysis, Induction motor, FFT, Condition monitoring

1. Introduction
In industries that utilize large-scale machinery, monitoring the condition of equipment is a crucial factor in enhancing the reliability and safety of the production process (Manikandan et al. 2021). One of the most widely used techniques is vibration analysis, which can serve as an important tool for decision-making regarding maintenance, repair, or replacement of machine components (Romanssini et al. 2023). The effective application of this technique can significantly reduce maintenance costs and extend the service life of machinery.

Vibration measurement is a critical component for detecting and diagnosing abnormalities in machinery. At present, piezoelectric accelerometers are widely accepted in this field due to their high accuracy (Yaghootkar et al. 2016). However, the cost of this type of sensor is relatively high, especially when multiple units need to be installed simultaneously, such as in wireless sensor network–based machine condition monitoring systems.

Advancements in embedded system technology and wireless sensor systems have led to the development of Micro-Electro-Mechanical Systems (MEMS) accelerometers, which provide a much lower-cost alternative for industrial vibration monitoring. This type of sensor integrates built-in signal conditioning circuitry, significantly reducing the overall system cost. In recent years, the market for MEMS accelerometers has grown rapidly, and the cost of these devices is expected to continue decreasing, making them increasingly suitable for industrial applications that require multi-point vibration monitoring. Furthermore, several research studies (Rehman et al. 2024; Son et al. 2016; Symes et al. 2025) have discussed the structural design of MEMS sensors, various considerations for installation, measurement principles, and performance evaluation in vibration detection.

MEMS accelerometer technology has therefore been widely adopted in certain industrial applications, such as the robotics industry, agricultural machinery industry, and the drone industry. However, the application of MEMS accelerometers for machine condition monitoring still lacks sufficient information to support the selection of the most effective MEMS accelerometer when specifications and prices are similar, in order to ensure suitability for practical machine condition monitoring. In (Son et al. 2016), three-axis and single-axis MEMS accelerometers were used together with an ultrasonic microphone to evaluate performance on a unidirectional vibration table. The results demonstrated that the sensors were able to accurately detect vibration frequencies and acoustic signals.

Although previous studies have explored the use of MEMS accelerometers in condition monitoring applications, several performance aspects remain insufficiently quantified. For example, (Jakobsen 2024) discussed low-cost MEMS-based monitoring systems incorporating multiple signal modalities, while (Scheffer and Girdhar 2004) emphasized the importance of mounting dynamics in vibration measurement accuracy. These works highlight important practical considerations; however, a tightly controlled and systematically quantified comparison between low-cost MEMS accelerometers and calibrated IEPE sensors under identical controlled sinusoidal excitation and synchronized acquisition conditions remains limited, particularly within the industrially relevant 10–100 Hz frequency range. Therefore, the objective of this study is to establish a structured and quantitative evaluation framework for assessing low-cost MEMS accelerometers against a calibrated IEPE reference sensor under controlled sinusoidal excitation and real motor operating conditions.

Specifically, this study aims to:
(1) Quantify sub-bin frequency tracking accuracy within the 10–100 Hz range.
(2) Evaluate narrowband RMS amplitude fidelity and its frequency dependency.
(3) Assess harmonic structure preservation through harmonic peak alignment and total harmonic distortion (THD).
(4) Compare noise performance using signal-to-noise ratio (SNR) derived from controlled spectral isolation.

While previous comparative studies often report general frequency agreement between MEMS and piezoelectric sensors, most focus on isolated performance indicators rather than a unified evaluation methodology. The present study differs in three principal aspects. First, frequency accuracy is quantified using sub-bin peak estimation under a shared clock acquisition system, minimizing timing bias. Second, amplitude deviation is evaluated using narrowband RMS ratios to reveal frequency-dependent sensitivity characteristics. Third, frequency error, harmonic alignment, THD, and SNR are integrated within a single multidimensional experimental framework, enabling a more comprehensive assessment of sensor suitability for frequency-domain machinery condition monitoring.

2. Problem Formulation

2.1 Performance Metrics

To evaluate the capability of low-cost MEMS accelerometers for rotating machinery condition monitoring, this study establishes a performance evaluation framework based on four key dimensions: frequency accuracy, amplitude accuracy, harmonic detection capability, and noise performance. A calibrated IEPE accelerometer was used as the reference sensor under identical excitation conditions and data acquisition systems, ensuring that any observed differences primarily reflect the behavior of the sensors and the measurement system.

(1) Frequency Tracking Accuracy

Frequency error is defined as the difference between the peak frequency measured by the MEMS sensor and the peak frequency measured by the reference IEPE sensor, as follows:

$$\Delta f = f_{MEMS} - f_{IEPE}$$

Where f_{MEMS} and f_{IEPE} are obtained from FFT analysis under identical sampling conditions.
In addition, the relative error expressed as a percentage was considered to reflect the accuracy of tracking the fundamental frequency within the range of 10–100 Hz, which is a critical band for rotating machinery analysis in industrial applications. This metric is important because accurate identification of rotational frequency and its harmonics forms the basis for fault diagnosis, such as unbalance and misalignment.

(2) Amplitude Fidelity

Although frequency accuracy reflects the capability to correctly identify peak locations, evaluating the severity of vibration also requires consideration of amplitude accuracy. Therefore, amplitude accuracy is defined in terms of the ratio of the narrowband RMS value around the fundamental frequency (±1 Hz) between the MEMS sensor and the IEPE sensor, as follows:

$$R_{amp} = \frac{RMS_{MEMS}}{RMS_{IEPE}}$$

A value that deviates from 1 reflects the frequency response characteristics of the measurement system, which may be influenced by the mechanical dynamics of the mounting method, the characteristics of the MEMS package, and the signal conditioning circuitry.

(3) Harmonic Detectability

To evaluate the linearity of the response and the capability to preserve the spectral structure of the signal, the error in the peak positions of the 2nd and 3rd harmonic components was examined as follows:

$$\Delta f_{harmonic} = f_{MEMS}^{(n)} - f_{IEPE}^{(n)}, n = 2,3$$

In addition, the Total Harmonic Distortion (THD) was calculated from the 2nd to 5th harmonic components to reflect the level of harmonic distortion in the measurement system. Accurate preservation of harmonic positions and orders is important for analyzing fault-related spectral features.

(4) Signal-to-Noise Ratio: SNR

The capability to detect low-amplitude spectral components was evaluated using the Signal-to-Noise Ratio (SNR), which was calculated as follows:

$$SNR = 20\, log_{10}(\frac{RMS_{signal}}{RMS_{noise}})$$

Where RMS_{signal} is the narrowband RMS value around the fundamental frequency and RMS_{noise} is the RMS value of the noise within the 0–500 Hz range after removing the bands around the main harmonics.

These four performance metrics collectively cover the key dimensions of vibration analysis in the frequency domain, including frequency positioning, quantitative amplitude accuracy, harmonic structure consistency, and noise limitations. Together, they form a systematic evaluation framework for comparing the performance of MEMS sensors with the reference IEPE sensor.

2.2 Evaluation Framework

To ensure that the performance evaluation of MEMS accelerometers is systematic and that the results can be clearly interpreted, this study establishes a comparison framework using a calibrated IEPE accelerometer as the reference standard. Both the MEMS and IEPE sensors were mounted at the same location on the shaker arm to ensure that they received identical excitation signals and to minimize errors arising from mounting position differences.

The excitation was defined as a periodic sine signal within the frequency range of 10–100 Hz, incremented in steps of 10 Hz. This frequency range is relevant to the analysis of rotating machinery in industrial applications. Data from all sensors were sampled at a rate of 2 kHz using the same data acquisition system and a shared clock source, ensuring that timing errors and jitter affected all signal channels equally. To control external interference factors, all MEMS sensors were mounted in magnetic bases with identical mass, and powered by batteries to reduce interference from 50 Hz AC power. The experimental setup and environmental conditions were kept consistent for all tests to ensure that any observed differences in frequency error, amplitude error, harmonic behavior, and noise performance directly reflect the characteristics of the measurement systems. Within this experimental framework, the evaluation focuses on a quantitative comparison between the MEMS and IEPE sensors in terms of frequency tracking accuracy, amplitude accuracy, preservation of harmonic structure, and noise limitations. These factors are critical for practical implementation in rotating machinery condition monitoring systems.

3. Methods

3.1 MEMS Sensor Characteristics

MEMS accelerometers are generally classified into piezoresistive and capacitive types (Alwazzan et al. 2025). This study focuses on capacitive MEMS devices, which consist of a proof mass suspended by micro-fabricated springs and interdigitated electrodes (Figure 1). Under acceleration, relative displacement of the proof mass induces differential capacitance variation, which is converted into a proportional electrical signal (Tez and Akin 2013). Compared to piezoelectric accelerometers, capacitive MEMS sensors offer compact size, low power consumption, and CMOS integration capability, making them suitable for distributed and wireless vibration monitoring. However, their performance depends on sensitivity, noise density, dynamic range, linearity, natural frequency, and damping characteristics. Recent studies have demonstrated the feasibility of MEMS accelerometers in vibration monitoring. (Rossi et al. 2023) reported measurement deviations below 5% compared to piezoelectric systems in rotating machinery. (Li et al. 2024) showed comparable low- to mid-frequency responses for low-cost MEMS sensors. (Huang et al. 2016), following ISO 16063-21 calibration procedures, achieved time- and frequency-domain results comparable to PZT sensors in milling monitoring. (Jiménez et al. 2016) demonstrated rotor-mounted MEMS accelerometers with agreement to eddy current displacement sensors under steady and transient conditions. (Ma et al. 2026) further improved resonant MEMS performance through structural frequency enhancement and active damping control to reduce vibration rectification error (VRE). Despite these advances, most studies emphasize application feasibility or isolated performance indicators. Limited research systematically addresses the metrological implications of low-cost MEMS accelerometers in industrial vibration monitoring, particularly regarding frequency-domain accuracy, harmonic preservation, amplitude fidelity, and signal-to-noise performance under tightly controlled comparative conditions. Theoretically, discrepancies between MEMS and IEPE measurements can be interpreted through the Frequency Response Function (FRF) of the combined sensor–mounting–structure system, where mounting stiffness, damping, packaging, and electronic noise may introduce frequency-dependent gain deviations and SNR limitations. Accordingly, this study presents a controlled, multidimensional frequency-domain evaluation of low-cost MEMS accelerometers relative to a calibrated IEPE reference under identical excitation and synchronized acquisition conditions.

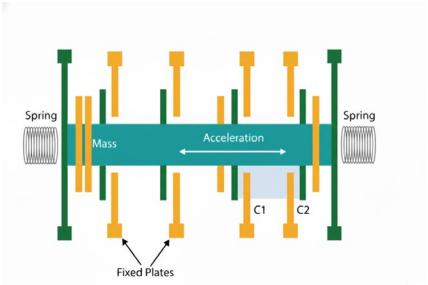

Figure 1 Structure of a MEMS accelerometer

This demonstrates the potential of MEMS for industrial applications. Key parameters considered when selecting an accelerometer include sensitivity, amplitude limit, shock limit, natural frequency, resolution, amplitude linearity, frequency range, and phase shift.

The key specifications of the IEPE reference sensor and the three MEMS accelerometers used in this study are summarized in Table 1. Key parameters considered when selecting an accelerometer include sensitivity, amplitude limit, shock limit, natural frequency, resolution, amplitude linearity, frequency range, and phase shift. Environmental factors and mounting methods—such as mounted resonant frequency and transverse sensitivity—may influence the frequency response of the measurement system and therefore must be taken into account in the experimental design.

Table 1. presents a comparison of the key specifications of the IEPE and MEMS sensors used in the experiment.

	IEPE Ref.	MEMS (V0)	MEMS (V1)	MEMS (V2)
Sensitivity (Vs=3V)	102mV/g	300mV/g	57mV/g	174mV/g
Frequency range (Hz)	1-9000 Hz	0.5-550 Hz	0.5-550 Hz	0.5-550 Hz
Amplitude limit (g)	+/-80	+/-3.6	+/-19	+/-6
Linearity	+/-1%	+/-0.3%	+/-0.3%	+/-0.2%
Shock limit (g)	5,000 g	10,000 g	10,000 g	10,000 g
Resolution (mg)	0.3mg	6.7mg	6.7mg	5.59mg

3.2 Experimental Setup

The experiment was conducted using a laboratory-scale electrodynamic vibration shaker driven by a linear power amplifier and controlled by a precision function generator producing sinusoidal excitation within the 10–100 Hz range. The excitation amplitude was maintained constant across all frequency steps to ensure consistent comparison. Four accelerometers were evaluated: one calibrated IEPE reference accelerometer (nominal sensitivity 102 mV/g; frequency range 1–9000 Hz) and three low-cost capacitive MEMS accelerometers (bandwidth 0.5–550 Hz). All sensors were mounted at the same location on the shaker arm to ensure identical mechanical excitation and minimize spatial variation. The MEMS sensors were installed in magnetic mounting bases of equal mass (approximately 50 g) to maintain consistent boundary conditions and comparable mounting stiffness. The IEPE sensor was mounted under equivalent structural conditions. Alternative mounting techniques, such as screw or adhesive attachment, were not investigated. Since mounting stiffness and structural resonance may affect the effective Frequency Response Function (FRF), evaluation of different mounting configurations remains a subject for future study. The overall experimental configuration used in this study is illustrated in Figure 2.

Figure 2. Test setup

3.3 Data Acquisition Configuration

All sensor signals were acquired using a LabJack T7 Pro data acquisition system equipped with a 24-bit sigma-delta ADC architecture. Data were sampled simultaneously at 2 kHz using a shared clock source to eliminate timing skew between channels. With this sampling rate, signals up to 500 Hz can be analyzed according to the Nyquist criterion, which is sufficient for the 10–100 Hz excitation range considered in this study. For each excitation frequency, approximately 27 seconds of data were recorded. The use of a common ADC and synchronized sampling ensured that any timing-related errors, such as jitter or drift, affected all channels equally, allowing observed differences to

primarily reflect sensor characteristics rather than acquisition artifacts. To reduce electromagnetic interference from 50 Hz AC power systems, all measurement equipment was powered by batteries during testing. In addition to controlled shaker experiments, measurements were conducted on an electric motor operating at 1000 RPM (approximately 16.7 Hz) to evaluate frequency-domain performance under practical operating conditions.

3.4 Excitation Procedure

The excitation was performed using a periodic sine signal within the frequency range of 10–100 Hz, with the frequency increased in 10 Hz increments at each step. Signals from all sensors were recorded simultaneously under identical conditions to enable consistent quantitative comparison between the MEMS and IEPE sensors. In addition to the controlled shaker tests, further experiments were conducted on a real electric motor operating at 1000 RPM (approximately 16.7 Hz in the frequency domain) to evaluate the capability of detecting the fundamental frequency and its harmonics under practical operating conditions. The excitation conditions in this study were limited to controlled sinusoidal signals and steady-state motor operation. Random or impulsive excitation scenarios, which may better represent transient fault conditions, were not included and remain subjects for future investigation (Figure 3).

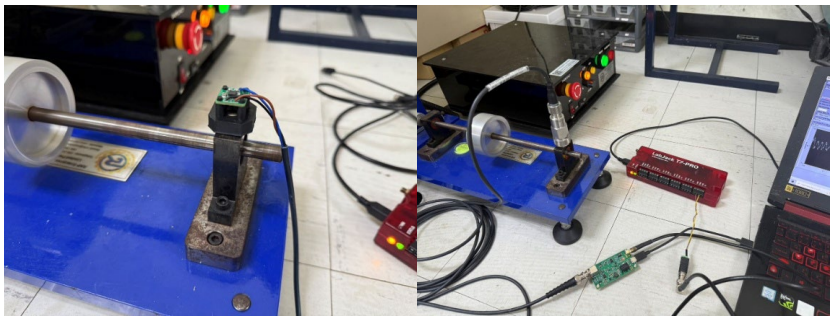

Figure 3. Electric Motor vibration monitoring setup

3.5 Signal Processing and Spectral Analysis

Signal processing was performed in Python in both the time and frequency domains. For each excitation condition, approximately 27 seconds of data were recorded at a sampling frequency of 2 kHz. A steady-state segment of 5 seconds from the central portion of the signal was selected for analysis to avoid transient effects at the beginning and end of the record. This corresponds to N = 10,000 samples and yields a theoretical frequency resolution of

$$\Delta f = \frac{F_S}{N} = 0.2Hz$$

Prior to spectral analysis, a Hann window was applied to the selected segment to reduce spectral leakage. The Fast Fourier Transform (FFT) was then computed without additional zero-padding. Peak frequencies were estimated using parabolic interpolation around the dominant spectral bin to obtain sub-bin frequency estimation. From the resulting spectrum, the performance metrics defined in Section 2 were calculated, including fundamental frequency error, narrowband RMS amplitude ratio (±1 Hz), total harmonic distortion (THD, 2–5), and signal-to-noise ratio (SNR) derived from harmonic-excluded noise bands.

4. Data Collection

4.1 Periodic Excitation Measurements

Controlled data acquisition was performed by exciting the shaker with sinusoidal signals in the 10–100 Hz range, incremented in 10 Hz steps. For each frequency level, approximately 27 seconds of data were recorded simultaneously from all sensors at a sampling rate of 2 kHz under identical mounting and acquisition conditions. From each dataset, a 5-second steady-state segment was selected for spectral analysis, ensuring consistent frequency resolution ($\Delta f = 0.2$ Hz) across all tests. This segment was used to compute the defined performance metrics, including fundamental frequency error, narrowband RMS amplitude ratio, total harmonic distortion (THD), and signal-to-noise ratio (SNR). All excitation levels were processed using the same segmentation, windowing, and spectral estimation procedures to maintain methodological consistency throughout the study. The present investigation emphasizes deterministic

comparison under tightly controlled laboratory conditions. Although repeated trials were not conducted at each frequency level, the consistent trends observed across the frequency sweep indicate stable measurement behavior under controlled laboratory conditions. A comprehensive statistical uncertainty analysis, including repeatability testing and confidence interval estimation, remains for future work.

4.2 Harmonic and Spectral Component Extraction

For the evaluation of spectral structure, the peaks corresponding to the fundamental frequency (1×) and the 2× and 3× harmonic components were identified from the frequency spectrum using sub-bin peak estimation as described in Section 3. The narrowband RMS values (±1 Hz) around each harmonic component were used to calculate the THD and were compared with the reference values obtained from the IEPE sensor to assess the capability of the MEMS sensors to preserve the harmonic structure of the signal.

4.3 Electric Motor Validation

In addition to the controlled shaker tests, additional data were collected from an electric motor in a laboratory environment operating at 1000 RPM, corresponding to a mechanical frequency of approximately 16.7 Hz. Signals from all three MEMS sensors were recorded and analyzed in both the time and frequency domains to evaluate their capability to detect the fundamental frequency and its harmonics under real operating conditions. The results from this test were used to verify the consistency of spectral behavior between the MEMS sensors and the reference sensor.

5. Results and Discussion

The experimental results under sinusoidal excitation in the 10–100 Hz range indicate that all three MEMS accelerometers consistently tracked the fundamental frequency. Representative time-domain acceleration responses at excitation frequencies of 20 Hz and 50 Hz are shown in Figure 4(a) and Figure 4(b), respectively. The measured peak frequencies closely followed the set excitation frequencies across all test points. The observed peak deviations remained significantly smaller than the theoretical FFT resolution ($\Delta f = 0.2$ Hz), confirming reliable frequency tracking performance. The use of parabolic interpolation reduced discretization effects associated with FFT bin spacing, enabling consistent sub-bin peak estimation. However, the achievable accuracy remains bounded by the acquisition resolution and signal-to-noise characteristics of the measurement system.

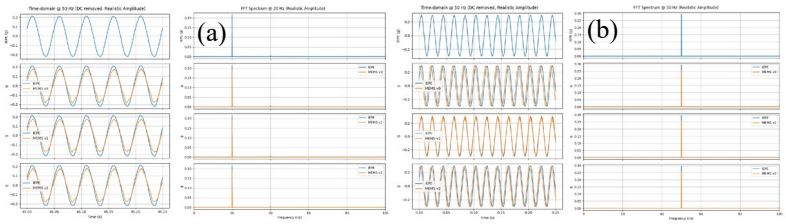

Figure 4. Measured acceleration responses *20* Hz and 50 Hz

The relationship between the excitation frequency and the measured peak frequency is shown in Figure *5*: Peak frequency vs excitation frequency, demonstrating nearly perfect agreement throughout the entire test range. The absolute frequency error and the percentage frequency error are presented in Figure *6*(a): Frequency error (Δf) and Figure *6*(b): Percent frequency error, respectively. The errors remain very small relative to the defined spectral resolution.

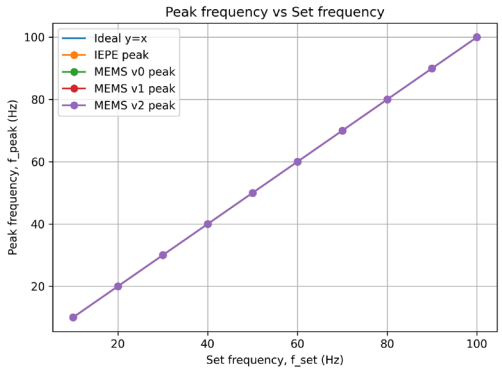

Figure 5. Peak frequency measured by the MEMS accelerometers and the reference (IEPE) accelerometer as a function of the set excitation frequency.

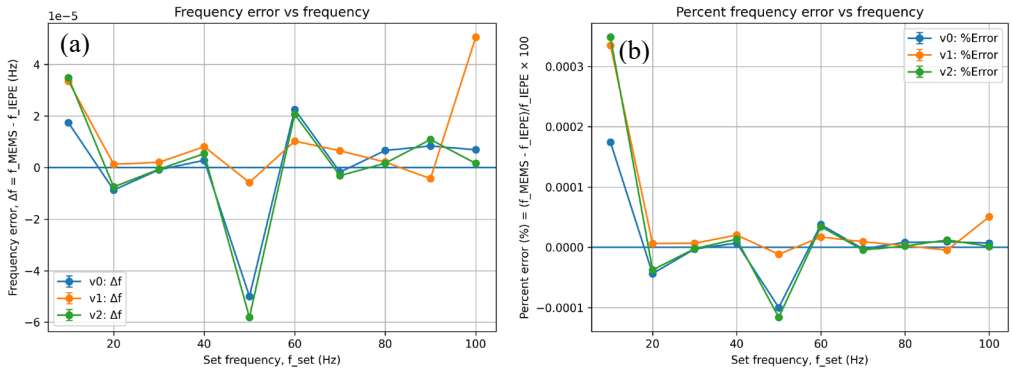

Figure 6. Frequency error of the MEMS accelerometers relative to the reference (IEPE) accelerometer: (a) Absolute error (Δf); (b) Percent error.

In terms of amplitude performance, the comparison of the narrowband RMS ratio is shown in Figure 7(a): RMS ratio and Figure 7(b): Sensitivity deviation. The results indicate that the amplitude deviation is dependent on the excitation frequency, reflecting the frequency response characteristics of the sensors and the mechanical mounting conditions. Although the MEMS sensors maintain accurate frequency positioning, noticeable amplitude differences are still observed within certain frequency ranges.

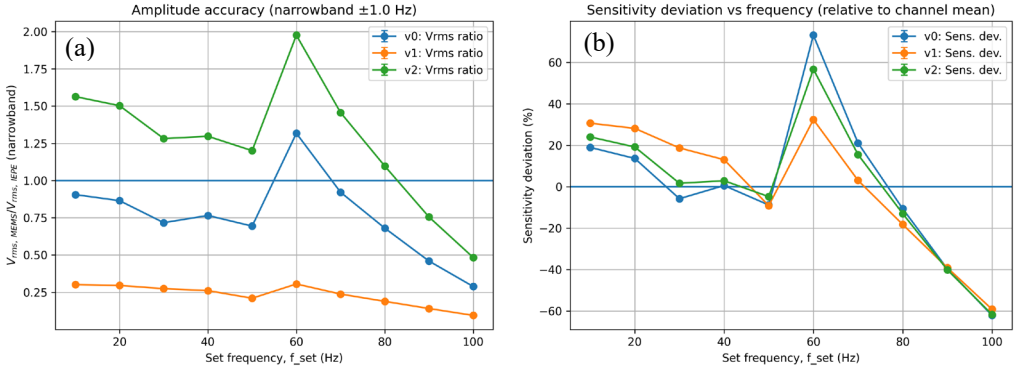

Figure 7. Amplitude performance comparison: (a) Narrowband RMS ratio; (b) Sensitivity deviation.

The harmonic structure of the signal is presented in Figure 8: FFT spectrum (1×, 2×, 3× components), where the main harmonic components align with those measured by the reference sensor. The harmonic position error is shown in Figure 9: Harmonic alignment error, which remains at a low level. However, the Total Harmonic Distortion values displayed in Figure 10: THD comparison reflect differences in the amplitude of certain harmonic components.

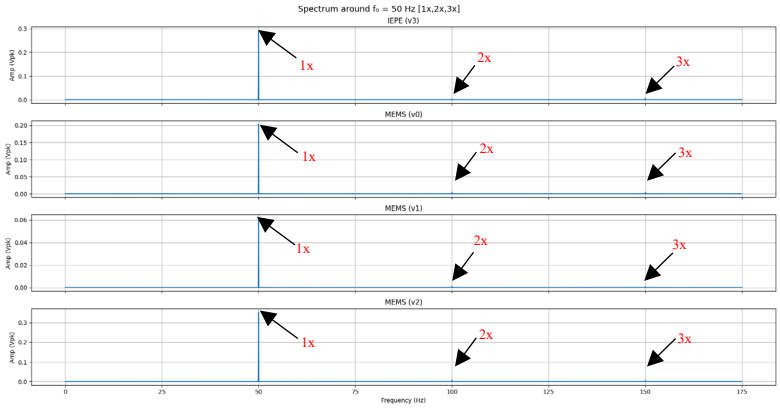

Figure 8. FFT spectra of the MEMS accelerometers and the reference (IEPE) accelerometer at 50 Hz, showing the fundamental (1×) and the second and third harmonics (2×, 3×).

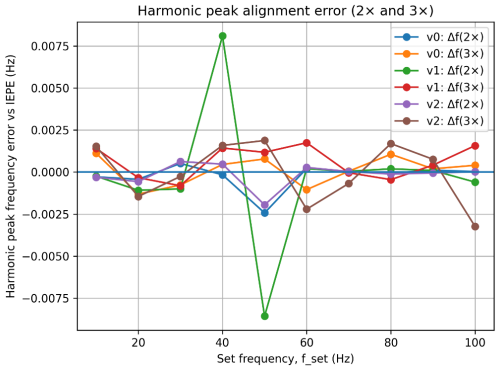

Figure 9. Harmonic peak alignment error at 2× and 3× for the MEMS accelerometers relative to the reference (IEPE) accelerometer versus set excitation frequency.

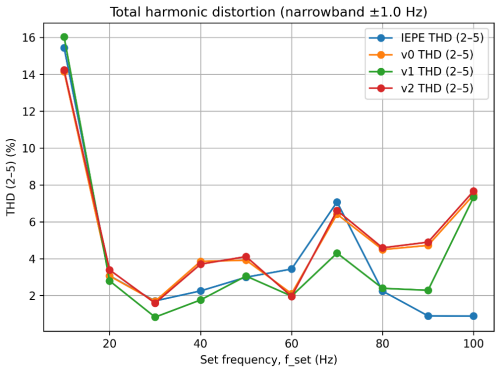

Figure 10. Total harmonic distortion (THD, 2–5) of the MEMS accelerometers and the reference (IEPE) accelerometer versus set excitation frequency (narrowband RMS, ±1 Hz).

The noise level of the measurement system is presented in Figure 11(a): Noise floor spectrum, and the Signal-to-Noise Ratio is shown in Figure 11 (b): SNR comparison. The MEMS sensors exhibit a higher noise floor than the IEPE sensor, resulting in lower SNR values across all frequency ranges. This may affect their capability to detect low-amplitude faults. When compared with typical manufacturer sensitivity tolerances for low-cost MEMS accelerometers (commonly ±10–20%), the observed amplitude deviations (up to ±50–70%) indicate that system-level effects—particularly mounting dynamics and structural resonance—contribute more significantly to gain variation than intrinsic sensor calibration error. From a diagnostic perspective, an SNR in the range of 25–35 dB allows reliable identification of dominant spectral components but may limit detection of low-amplitude fault-related sidebands, especially in early-stage fault conditions where signal levels approach the noise floor.

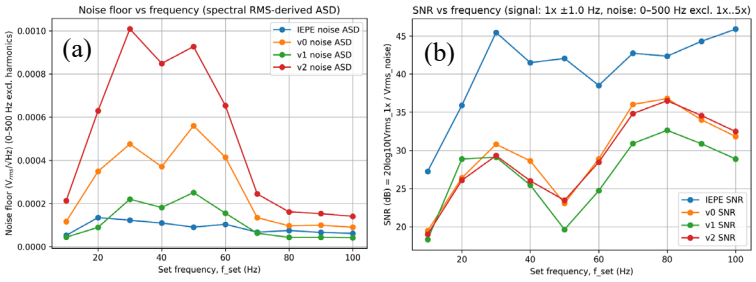

Figure 11. Noise performance of the MEMS and reference (IEPE) accelerometers versus excitation frequency: (a) Estimated noise floor; (b) Signal-to-noise ratio (SNR).

To evaluate performance under real operating conditions, tests were conducted on an electric motor running at 1000 RPM. The installation setup is shown in Figure 3: Electric Motor vibration monitoring setup, and the measured spectrum is presented in Figure 12 : Electric Motor vibration measured by MEMS accelerometers at 1000 rpm. The results indicate that the MEMS sensors were able to detect the fundamental frequency (~16.7 Hz) and the second harmonic (~33 Hz) consistently with the reference sensor, although some amplitude differences were observed. These findings support the practical feasibility, particularly in applications where frequency identification is more critical than amplitude accuracy.

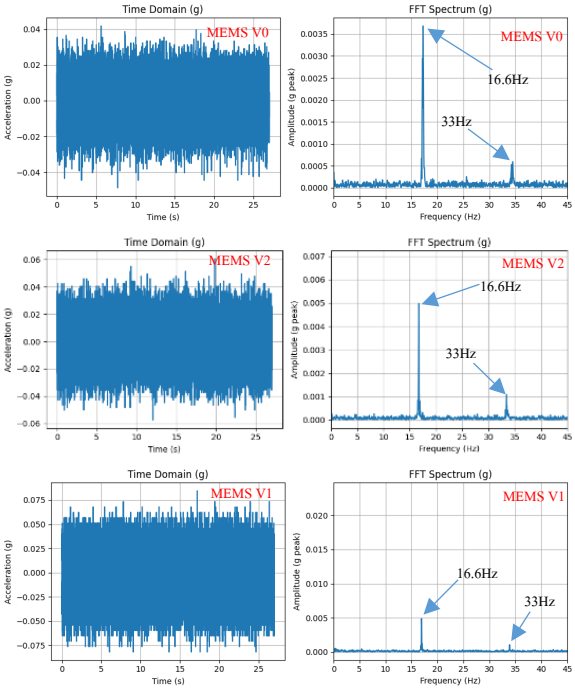

Figure 12. Electric Motor vibration measured by the MEMS accelerometers at speed of 1000 rpm

6. Conclusion

This research evaluates the performance of low-cost MEMS accelerometers by comparing them with a calibrated IEPE reference sensor under controlled sinusoidal excitation in the 10–100 Hz range and steady-state operation of an electric motor. Under the spectral resolution constraint of $\Delta f = 0.2$ Hz, the MEMS sensors were able to consistently track the fundamental frequency and harmonics, demonstrating stable frequency identification capability in the frequency domain. During motor operation at 1000 rpm (approximately 16.7 Hz), the MEMS devices were able to accurately detect the fundamental rotational frequency and the second harmonic (approximately 33 Hz) in agreement with the reference sensor. Although amplitude deviations were observed, the spectral peak locations remained within the specified resolution limit, confirming the reliability of rotational frequency identification.

The narrowband RMS deviations were frequency-dependent and reached up to approximately ±50–70%, exceeding the typical sensitivity tolerance specified by manufacturers (±10–20%). These deviations reflect variations in the overall system frequency response function (FRF) of the combined sensor–mounting–structure assembly rather than intrinsic errors of the sensor itself. This indicates that mounting dynamics and structural coupling are the primary factors determining gain accuracy.

The noise analysis showed that the MEMS devices exhibited lower Signal-to-Noise Ratio (SNR) values (25–35 dB) compared to the IEPE sensor (>40 dB). Although the main spectral components could still be identified within this range, the reduced noise margin may limit the ability to detect low-amplitude sidebands associated with early-stage damage. Overall, the results indicate a trade-off between the robustness of frequency identification and the quantitative accuracy of amplitude in vibration monitoring systems employing low-cost MEMS sensors. The main contribution of this research is the establishment of a multidimensional evaluation framework in the frequency domain, integrating spectral resolution constraints, harmonic persistence, amplitude accuracy, and noise characteristics under identical data acquisition conditions. This framework helps define the practical performance boundaries and supports principled decision-making in sensor selection and system design for industrial machinery condition monitoring applications.

Practical Recommendations

For industrial practitioners, low-cost MEMS accelerometers are suitable for applications primarily focused on frequency identification, such as detecting rotational speed and harmonic components. However, when quantitative amplitude assessment or compliance with vibration severity standards is required, frequency-dependent calibration relative to a reference sensor is recommended prior to deployment. In configurations using magnetic mounting, additional attention should be given to potential gain variation introduced by mounting stiffness and structural resonance.

For system designers, applications requiring detection of low-amplitude early-stage faults should consider acquisition configurations capable of achieving SNR levels above approximately 35–40 dB to maintain sufficient diagnostic margin.

Research Recommendations

Future investigations should prioritize (1) systematic Frequency Response Function (FRF) characterization under multiple mounting configurations, (2) repeatability and statistical uncertainty quantification, and (3) evaluation under non-sinusoidal excitation such as impulsive or random vibration to better represent real fault conditions.

References

Alwazzan, O.A.S., Fathalilou, M. and Rezazadeh, G., Coupled nonlinear modeling of a novel high-sensitivity MEMS capacitive accelerometer enhanced by tilted pillars, Applied Mathematical Modelling, vol. 140, p. 115897, April 2025.

Huang, C.-Y., Lee, R.-M., Yang, S.-K., Implement of low cost MEMS accelerometers for vibration monitoring of milling process, IEEE International Conference on Advanced Manufacturing, pp. 1–4, 2016.

Jakobsen, M.O., Low cost MEMS accelerometer and microphone based condition monitoring sensor, with LoRa and Bluetooth low energy radio, HardwareX, vol. 18, p. e00525, 2024.

Jiménez, S., Cole, M.O.T., Keogh, P.S., Vibration sensing in smart machine rotors using internal MEMS accelerometers, Journal of Sound and Vibration, vol. 377, pp. 58–75, 2016.

Li, X., et al., Performance evaluation of low-cost MEMS accelerometers for vibration monitoring applications, Mechanical Systems and Signal Processing, vol. 190, p. 110123, 2024.

Ma, K., et al., Vibration performance analysis and improvement of MEMS resonant accelerometers, IEEE Transactions on Industrial Electronics, vol. 73, no. 2, pp. 1234–1245, 2026.

Manikandan, K.G., Pannirselvam, K., Kenned, J.J. and Kumar, C.S., Investigations on suitability of MEMS based accelerometer for vibration measurements, Materials Today: Proceedings, vol. 45, no. 7, pp. 6183–6192, 2021.

Rehman, S.U., Usman, M., Toor, M.H.Y. and Hussaini, Q.A., Advancing structural health monitoring: A vibration-based IoT approach for remote real-time systems, Sensors and Actuators A: Physical, vol. 365, p. 114863, 2024.

Romanssini, M., de Aguirre, P.C.C., Compassi-Severo, L. and Girardi, A.G., A review on vibration monitoring techniques for predictive maintenance of rotating machinery, Eng, vol. 4, no. 3, pp. 1797–1817, June 2023.

Rossi, A., Bocchetta, G., Botta, F. and Scorza, A., Accuracy characterization of a MEMS accelerometer for vibration monitoring in a rotating framework, Applied Sciences, vol. 13, p. 5070, 2023.

Scheffer, C. and Girdhar, P., Practical Machinery Vibration Analysis and Predictive Maintenance, Elsevier, Amsterdam, The Netherlands, 2004.

Son, J.-D., Ahn, B.-H., Ha, J.-M. and Choi, B.-K., An availability of MEMS-based accelerometers and current sensors in machinery fault diagnosis, Measurement, vol. 94, pp. 680–691, 2016.

Symes, R.W., Varley, R.J., St John, N., Ibrahim, M. and Joosten, M.W., Comparative analysis of MEMS (micro-electro-mechanical sensor) and IEPE (integrated electronics piezo-electric) accelerometers for measurement of wide spectrum damping, Measurement, vol. 242, p. 115963, 2025.

Tez, S. and Akin, T., Fabrication of a sandwich type three axis capacitive MEMS accelerometer, Proceedings of the IEEE Sensors Conference, Baltimore, MD, USA, November 3–6, 2013, pp. 1–4.

Yaghootkar, B., Azimi, S. and Bahreyni, B., Wideband piezoelectric MEMS vibration sensor, Proceedings of the IEEE Sensors Conference, Orlando, FL, USA, October 30–November 2, 2016.

Biographies

Wetis Klingram is a master's student in Industrial Engineering at Suranaree University of Technology, Thailand. His research interests include vibration-based condition monitoring, MEMS sensor systems, signal processing using FFT, and predictive maintenance of rotating machinery. He is currently working on the development of a low-cost vibration measurement system for induction motor fault diagnosis and performance evaluation.

Nattawat Pinrath, Ph.D., is a Lecturer in the School of Industrial Engineering at Suranaree University of Technology, Thailand. His research interests include manufacturing systems, maintenance engineering, data analytics, and industrial sensor applications.